ON THE USE OF IMPLICIT AND ITERATIVE METHODS FOR THE TIME INTEGRATION OF THE WAVE EQUATION

YOSHIO KURIHARA*

Geophysical Fluid Dynamics Laboratory, U.S. Weather Bureau, Washington, D.C.

ABSTRACT

The numerical properties of the trapezoidal implicit, the backward implicit, and partly implicit methods are investigated. The computational stability of these methods, the selective damping of waves, and the accuracy of the predicted wave are discussed primarily for wave equations in the simple form. Then, their applicability to the integration of the primitive equations is considered for a system of linearized equations.

The characteristic features of four iterative methods, each of which consists of a predictor and a corrector to be used only once, are also described.

1. INTRODUCTION

The very short-period oscillations inevitably undergone by any meteorological quantity predicted by a system of primitive equations are principally noise, if an atmospheric model is designed so as to forecast a large-scale and slowly moving meteorological wave. The noise appears as high-frequency gravitational waves. In this paper the words "gravitational wave" will be used in this sense.

It is necessary to suppress the noise. Otherwise, an important meteorological wave can be masked by it. The problem of initialization of data has been studied to find a way to reduce the amplitude of noise (e.g., Hinkelmann [4], Phillips [7]). This can be attained by an appropriate adjustment between the fields of wind and pressure. However, the control of noise which may arise after the initial time has not yet been achieved. This problem is presumably serious when a model of the moist atmosphere is dealt with or when the influence of orography is taken into consideration. Namely, if a rapidly changeable process such as the release of latent heat due to condensation of water vapor is included without care in a prognostic equation, the maintained adjustment between the two fields will be destroyed and noise will be excited. Similarly, the motion which is forced by mountains is a source of noise too. In addition, noise will be amplified if the procedure of numerical integration of the primitive equations does not satisfy the condition for computational stability. In the case of the "leapfrog" method, which is widely used and is also called the centered-difference method, this condition places an upper limit on the time interval of the marching process. The time interval thus specified is very small as compared with the characteristic time of the meteorological wave.

On the other hand, it has been known that a stable integration of wave equations can be made without any restriction on the time interval by making use of implicit methods (Richtmyer [10]). Furthermore, it is possible to establish an implicit scheme which causes damping of the wave. The degree of this damping effect differs with the period of the wave, just as finite differencing in space has some selective properties for waves with different scales. Consequently, the difficulties associated with the occurrence or the growth of noise may be overcome to some degree with an implicit method. Many implicit schemes have been discussed; however those to be considered in this paper are the relatively simple ones. The purpose of this study is to investigate the numerical properties of these schemes when they are used for integrating the wave equation. In particular, consideration will be given to how high-frequency waves behave when a large time interval is taken and how selective the damping of the wave is with period.

The discussions in section 3 relative to the applicability of implicit methods to the integration of the primitive equations are based on a system of linearized equations without viscosity. The actual quadratic nature of the equations, from which arise problems of nonlinear instability (Phillips [8]) and of the interaction between meteorological wave and noise which reduce the accuracy of the prediction of the former wave, will not be considered in this paper.

A few articles concerning the use of implicit methods have been published in Russian journals (e.g., Tseng Ch'ing-ts'un [12], Bortnikov [1], Turianskaĭa [11]). The computational instability of one of these methods will be pointed out.

The implicit methods require one to solve a non-trivial equation for the values at a new time level. One such method is an iterative procedure (e.g., a trapezoidal implicit method with an iterative scheme used by Uusitalo

*On leave from the Meteorological Research Institute, Tokyo, Japan.

[13] and Veronis [14]). Generally speaking, an iterative method consists of obtaining a tentative value by a predictor and correcting it recursively by a corrector. In section 4, methods in which a corrector is used only once will be presented. These methods have a property of selectively damping the wave solutions. One of them, which will be referred to in this paper as the Euler-backward method, is being used for the time integration of a general circulation model at the University of California, Los Angeles. Recently, the integration of the primitive equations has been done with the so-called improved Euler-Cauchy method (Grammeltvedt [3]). Eliassen [2] has described the built-in selective damping of this method. It should be remarked that this property is not derived from the finite differencing in time, but results from non-centered finite differencing in space. In this respect, it is different in quality from the selective damping to be discussed in this paper.

If more than two time levels are associated with a scheme of integration for equations of the first order, computational modes will appear which may give rise to instabilities in numerical integration. Some methods can eliminate or damp this fictitious mode (e.g., Miyakoda [6], Phillips [9], Lilly [5]). It seems that the leapfrog-trapezoidal method discussed in section 4 is very useful for suppressing it.

2. PROPERTIES OF IMPLICIT SCHEMES AND THE LEAP-FROG METHOD IN THE TIME INTEGRATION OF THE WAVE EQUATION

The equation for a quantity, h, which propagates as a sinusoidal wave does with wavelength, L, and phase velocity, C, is

$$\frac{\partial h}{\partial t}=-ivch \tag{2.1}$$

where

$$\nu=2\pi/L,\ i=\sqrt{-1}.$$

The advection of the quantity is accurately shown by the right-hand side of (2.1). When we use a spectrum method, in which a wave is represented by functions and a space derivative is obtained analytically, an estimation of the advection is accurate. In the following discussions, we assume that the advection takes an accurate value, unless we mention especially finite differencing in space. This will make the properties of time integration schemes clear. Accordingly, the results of the investigations can be applied to the schemes in which a spectrum method, e.g., a Fourier series, is adopted. If a grid method is used to compute the space derivatives, the tendency equation will be changed. In case of the centered space differences, however, the change in (2.1) is only a modification of phase velocity. Therefore, we can apply the results to be obtained also to the schemes with centered space differences, if a modification of (2.1) is taken into consideration.

TWO TIME-LEVELS SCHEME

We consider the cases where two time-levels, τ and $\tau+1$, are used in integrating (2.1) numerically and the scheme of computation takes the form

$$h^{\tau+1}-h^{\tau}=-i\alpha h^{\tau+1}-i\beta h^{\tau} \tag{2.2}$$

where α and β are coefficients at our disposal under the condition $\alpha+\beta=\nu c(\Delta t)$. Δt is the time interval between two time-levels. The so-called amplification matrix of (2.2) is $|(1-i\beta)/(1+i\alpha)|$. Then, provided the magnitude of the eigenvalue of the above single element matrix is equal to or less than one, the scheme (2.2) is computationally stable.

Let $\lambda=R\exp i\vartheta$ be the eigenvalue. In the case of a two time-levels scheme, there is only one eigenvalue: namely, no computational mode arises out of the process of numerical integration. In the above expression of λ, R denotes the amplifying rate, which is, of course, fictitious. The phase velocity of the computed physical mode is $-\vartheta/\nu\Delta t$.

When α is zero in (2.2), a forward time difference scheme (Method 0) is obtained. Hereafter, an Arabic number will be used to identify an explicit method in contrast to an alphabetic letter for identification of an implicit scheme. The values of ϑ and R for a specified value of β are

$$\vartheta=\tan^{-1}(-\beta)$$

$$R=(\cos\vartheta)^{-1}$$

using the above ϑ, respectively.

The trace of the eigenvalue in the complex plane as a function of β is shown in figure 2.1. As R is always larger than one, this explicit scheme is absolutely unstable. It is known that an explicit scheme is conditionally stable if we use noncentered, upstream differences in the computation of the space derivatives (e.g., Richtmyer [10]). In this case, a computation scheme takes a different form from (2.2).

We shall now discuss the properties of two implicit schemes for representing (2.2).

Method A (backward implicit method).—Putting $\beta=0$ in (2.2) we have

$$h^{\tau+1}-h^{\tau}=-i\alpha h^{\tau+1}. \tag{2.3}$$

In this case, ϑ and R for a specified value of α are

$$\vartheta=\tan^{-1}(-\alpha)$$

$$R=\cos\vartheta, \text{ using the above } \vartheta.$$

Figure 2.2 shows the trace of λ on the complex plane. This method is absolutely stable and causes damping of a wave. In the limit of large $|\alpha|$, a wave will be completely damped out. It is also seen that the phase difference of a wave at two time-levels is at most $\pi/2$, i.e., below one-fourth of wavelength in either direction.

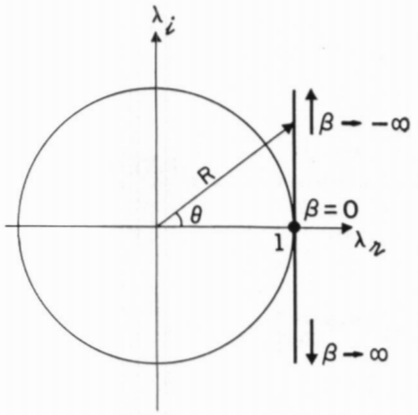

FIGURE 2.1.—Trace of eigenvalue for Method O (forward explicit method). Eigenvalue, $\lambda_r+i\lambda_i$, of the amplification matrix (single element) of $h^{\tau+1}-h^{\tau}=-i\beta h^{\tau}$ is shown on the complex plane. For a given parameter β, R represents the magnitude of eigenvalue, i.e., amplifying rate, and ϑ is the phase angle of eigenvalue.

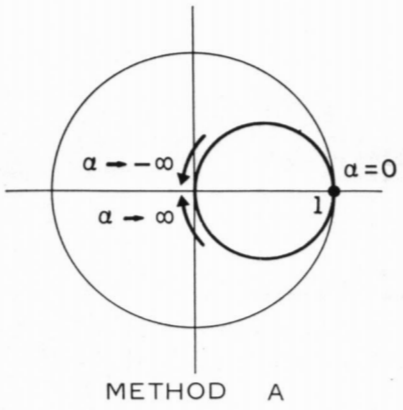

FIGURE 2.2.—Trace of eigenvalue for Method A (backward implicit method). Eigenvalue of the amplification matrix of (2.3) is shown on the complex plane. α is a parameter. In the limit of large $|\alpha|$, a wave is completely damped out.

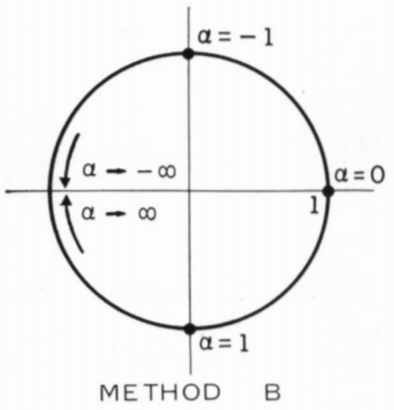

FIGURE 2.3.—Trace of eigenvalue for Method B (trapezoidal implicit method). Eigenvalue of the amplification matrix of (2.4) is shown on the complex plane. α is a parameter. An amplitude of wave does not change for any value of α, since $R=1$ always. In the limit of large $|\alpha|$, a wave is shifted by half a wavelength.

Method B (trapezoidal implicit method).—This scheme is obtained by putting $\beta=\alpha$ in (2.2),

$$h^{\tau+1}-h^{\tau}=-i\alpha h^{\tau+1}-i\alpha h^{\tau}. \tag{2.4}$$

In this case, ϑ is to be obtained as a solution of

$$-\sin\vartheta/(1+\cos\vartheta)=\alpha,$$

and $R=1$.

The trace of λ is shown in figure 2.3. This scheme is neutral in the sense that it neither amplifies nor damps a wave. The eigenvalue for large $|\alpha|$ approaches -1. Thus, the phase of a wave will be shifted by π, i.e., half a wavelength, in one time step if $|\alpha|$ is infinitely large.

We shall now give examples of numerical integration with the use of the above two implicit methods. A system of equations admitting only inertia oscillations is

$$\begin{cases}\dfrac{\partial u}{\partial t}=fv\\[2ex] \dfrac{\partial v}{\partial t}=-fu\end{cases}$$

where u is an eastward wind velocity, v is a northward wind velocity, and f is the Coriolis parameter. These equations are rewritten in the form of (2.1),

$$\frac{\partial w}{\partial t}=-ifw \tag{2.5}$$

where

$$w=u+iv.$$

A time integration of (2.5) was done by the formulas:

$$w^{\tau+1}-w^{\tau}=-if\Delta t w^{\tau+1} \qquad \text{(Method A)}$$

and

$$w^{\tau+1}-w^{\tau}=-if\frac{\Delta t}{2}w^{\tau+1}-if\frac{\Delta t}{2}w^{\tau}, \quad \text{(Method B)}$$

starting from the given initial value $w^0=u^0=1$, and assuming $f=\pi/9$ (hr.$^{-1}$). The period of oscillation is then 18 hr. Figure 2.4 shows single-step predictions of u for various values of Δt. To use long time steps in Method A gives complete damping, i.e., $u^1=0$; while with Method B, $u^1=-u^0=-1$ and $v^1=-v^0=0$. Although there exists no damping effect in Method B, the error in the phase velocity will make a prediction meaningless if the time step chosen is larger than about one-sixth of a period of the wave. In figure 2.5 are shown predictions of u, in which Methods A, B, and explicit leapfrog method (Method 1) were repeatedly used, respectively, with a time step of one hour. The damping effect in Method A is clearly seen.

The general case of (2.2) will be referred to as Method C.

Method C. (partly implicit method).—For convenience, (2.2) is repeated:

$$h^{\tau+1}-h^{\tau}=-i\alpha h^{\tau+1}-i\beta h^{\tau} \tag{2.2}$$

In this case the real and imaginary parts of the eigenvalue are

$$\lambda_{real}=(1-\alpha\beta)/(1+\alpha^2)$$

$$\lambda_{imag}=-(\alpha+\beta)/(1+\alpha^2)$$

respectively. Accordingly, the magnitude of λ is

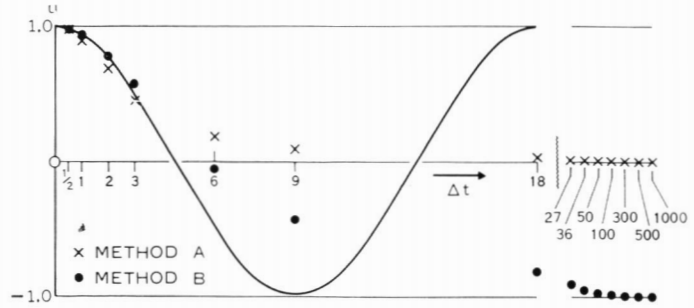

FIGURE 2.4.—Single-step prediction of inertia oscillation with various time intervals (Δt in hr.). u at $t=\Delta t$ is plotted.

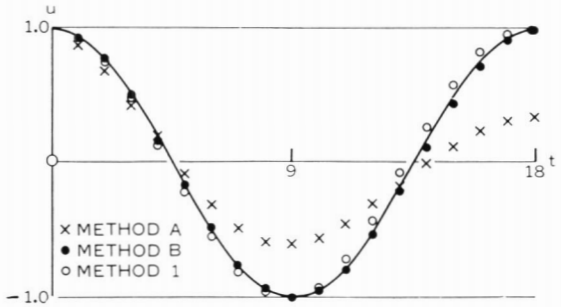

FIGURE 2.5.—Prediction of inertia oscillation with $\Delta t=1$ hr. u is plotted.

$$|\lambda|=[(1+\alpha^2)(1+\beta^2)]^{1/2}/(1+\alpha^2)$$

The computational stability condition for (2.2) is, therefore,

$$|\beta|\leq|\alpha|$$

We use this condition in section 3 where we investigate the computational stability of the two time-levels integration scheme in which some terms of the primitive equations take implicit form and others take explicit form.

THREE TIME-LEVELS SCHEME

Now consideration will be given to the three time-levels formula of the following form

$$h^{\tau+1}-h^{\tau-1}=-i\alpha h^{\tau+1}-i\beta h^{\tau} \tag{2.6}$$

We do not discuss a general three time-levels scheme, but consider only a combined form of the leapfrog and an implicit method. The amplification matrix of the above formula is

$$\begin{vmatrix} -\dfrac{i\beta}{1+i\alpha} & \dfrac{1}{1+i\alpha} \\ 1 & 0 \end{vmatrix}$$

The eigenvalues of the above matrix are obtained as solutions (see Appendix 2) of the equation

$$(1+i\alpha)\lambda^2+i\beta\lambda-1=0. \tag{2.7}$$

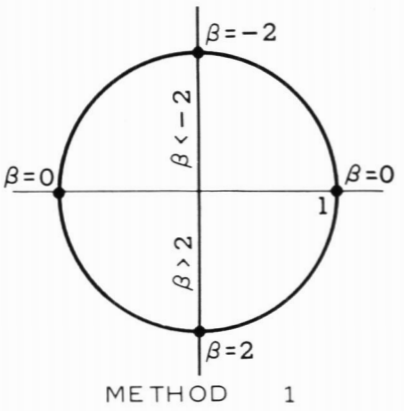

FIGURE 2.6.—Trace of eigenvalue for Method 1 (leapfrog method). Eigenvalues of the amplification matrix of (2.8) are shown on the complex plane. β is a parameter. The right half of the unit circle corresponds to the computed physical mode and the left half to the computational mode. If $|\beta|<2$, one of the two eigenvalues represents the former mode and the other does the latter mode. If $|\beta|>2$, two eigenvalues are on the axis of $\lambda_r=0$ and one of them is outside the unit circle, i.e., the scheme is computationally unstable.

One of two solutions applies to amplification rate and phase velocity of the physical mode, and the other describes those of the so-called computational mode. (Note that the amplification rate and phase velocity of the true physical mode are unity and c, respectively, as defined by (2.1).) In the analysis of λ, we will use either of the two forms: $\lambda=\lambda_r+i\lambda_i$ or $\lambda=R\exp i\vartheta$. Suffix 1 or 2 may be attached to λ, R or ϑ to denote the above-mentioned two modes, if necessary. The computational stability condition for (2.6) is that both R_1 and R_2 should be equal to or less than one. In the following, a special case and the general case of (2.6) will be examined separately.

Method 1 (leapfrog method).—This scheme is obtained by putting $\alpha=0$ in (2.6):

$$h^{\tau+1}-h^{\tau-1}=-i\beta h^{\tau}. \tag{2.8}$$

It is well known that, if $|\beta|<2$

$$\lambda_r=\pm\sqrt{1-(\beta/2)^2}$$

$$\lambda_i=-\beta/2$$

and

$$|\lambda_1|=|\lambda_2|=1;$$

while if $|\beta|>2$

$$\lambda_r=0$$

$$\lambda_i=-\beta/2\pm\sqrt{(\beta/2)^2-1}$$

and one of $|\lambda_{1,2}|$ is larger than one. As a consequence the computational stability condition is met if $|\beta|<2$. Figure 2.6 shows the trace of λ. The right half of the unit circle

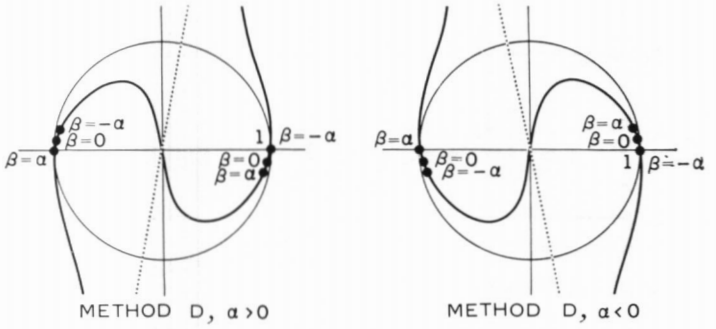

FIGURE 2.7.—Trace of eigenvalue for Method D (three time-levels, partly implicit method). Eigenvalues of the amplification matrix of (2.6) are shown on the complex plane separately for the cases $\alpha>0$ and $\alpha<0$. In each figure, the trace approaches to the dotted line when $\beta\to\pm\infty$. If $|\beta|<|\alpha|$, two eigenvalues are inside the unit circle, i.e., the scheme is computationally stable.

corresponds to the computed physical mode and the left half to the computational mode when $|\beta|<2$. If we define b by $b=|\beta|/2$, amplification rates, R_1 and R_2, and the ratio of the phase velocity of the computed value to true one, $-\vartheta_1/b$ and $-\vartheta_2/b$, can be estimated as a function of b. These are illustrated in figure 4.1. It is seen that the computed physical mode will move a little faster than the true physical mode. This tendency can be recognized in figure 2.5.

Method D (partly implicit method).—The general case of (2.6) will be treated here,

$$h^{\tau+1}-h^{\tau-1}=-i\alpha h^{\tau+1}-i\beta h^{\tau}$$

From $\lambda=R\exp i\vartheta$ and (2.7) we have

$$R^2(\cos 2\vartheta-\alpha\sin 2\vartheta)-R\beta\sin\vartheta-1=0$$

$$R^2(\sin 2\vartheta+\alpha\cos 2\vartheta)+R\beta\cos\vartheta=0.$$

From these, a relation involving R, ϑ, and α is obtained,

$$R^2=1/(1-\alpha\tan\vartheta).$$

As R is real, ϑ is undefined within some ranges, i.e.

$$\tan^{-1}\frac{1}{\alpha}<\vartheta<\frac{\pi}{2}\text{ and }\tan^{-1}\frac{1}{\alpha}+\pi<\vartheta<\frac{3\pi}{2}\text{ if }\alpha>0$$

$$-\frac{\pi}{2}<\vartheta<\tan^{-1}\frac{1}{\alpha}\text{ and }-\frac{3\pi}{2}<\vartheta<\tan^{-1}\frac{1}{\alpha}-\pi\text{ if }\alpha<0.$$

Furthermore, it is seen that when $\alpha>0$

$$\left.\begin{aligned}-\frac{\pi}{2}<\vartheta_1<0\\ \frac{\pi}{2}<\vartheta_2<\pi\end{aligned}\right\}\text{ if }|\beta|<|\alpha|$$

One of the $\vartheta_{1,2}$ is out of the above ranges if $|\beta|>|\alpha|$. When $\alpha<0$

$$\left.\begin{aligned}0<\vartheta_1<\frac{\pi}{2}\\ \pi<\vartheta_2<\frac{3\pi}{2}\end{aligned}\right\}\text{ if }|\beta|<|\alpha|.$$

One of the $\vartheta_{1,2}$ is out of the above ranges if $|\beta|>|\alpha|$. The trace of the eigenvalues, in which the parameter is β, is shown separately for the cases $\alpha>0$ and $\alpha<0$ in figure 2.7. Summarizing the results, we can conclude that both R_1 and R_2 are smaller than one if $|\beta|<|\alpha|$; otherwise, one of R_i becomes larger than one. Method D is, therefore, conditionally stable.

3. APPLICATION OF IMPLICIT SCHEMES FOR EQUATIONS OF ATMOSPHERIC WAVES

In this section, the problem of the time integration of the primitive equations with an implicit scheme will be considered by using the results obtained in the previous section.

Equations (3.1), a system of linearized perturbation equations, are derived from the assumptions that $\varphi=H(y)g+\phi(x)$ and $-(g/f)\partial H/\partial y=U$, where φ is geopotential, H mean height of the atmosphere as a function of y, g acceleration of gravity, ϕ perturbation of geopotential, f the Coriolis parameter, and U is a constant zonal wind in the x-direction in a rectangular system of coordinates:

$$\left.\begin{aligned}\frac{\partial u}{\partial t}+U\frac{\partial u}{\partial x}&=fv-\frac{\partial\phi}{\partial x}\\ \frac{\partial v}{\partial t}+U\frac{\partial v}{\partial x}&=-fu\\ \frac{\partial\phi}{\partial t}+U\frac{\partial\phi}{\partial x}&=fUv-gH\frac{\partial u}{\partial x}\end{aligned}\right\}\qquad(3.1)$$

Here u and v are x and y components of the perturbation wind velocity. Solutions of (3.1) are given by

$$\left.\begin{aligned}u&=\sum_{i=1}^{3}u_i, & u_i&=\phi_i\frac{\nu^2(U-c_i)}{f^2-(U-c_i)^2\nu^2}\\ v&=\sum_{i=1}^{3}v_i, & v_i&=\phi_i\frac{i\nu f}{f^2-(U-c_i)^2\nu^2}\\ \phi&=\sum_{i=1}^{3}\phi_i, & \phi_i&=S_i\exp\left[i\nu(x-c_it)\right]\end{aligned}\right\}\qquad(3.2)$$

where $\nu=2\pi/L$, L is the wavelength, $c_i(i=1, 2, 3)$ are the three phase velocities and S_i are amplitudes of three waves. The c_i should be obtained as roots of the equation

$$(U-c)^3-gH(U-c)+\frac{f^2}{\nu^2}c=0.$$

For the ordinary values of f, g, H, U, and ν, these are written

TABLE 3.1.—*Phase velocities* (c_1, c_2, *and* c_3) *and* νc_i. *In (3.3),* $U=50$ *m./sec.,* $gH=8\times10^4$ *m.²/sec.² and* f *at the 45° latitude are assumed.*

Wavelength (km.)	c_1 (m./sec.)	c_2 (m./sec.)	c_3 (m./sec.)	νc_1 (sec.$^{-1}$)	νc_2 (sec.$^{-1}$)	$\lvert\nu c_3\rvert$ (sec.$^{-1}$)
250	49.99	332.9	−232.9	$1.256\ 10^{-3}$	$8.366\ 10^{-3}$	$5.853\ 10^{-3}$
500	49.96	333.0	−232.9	$6.278\ 10^{-4}$	4.184	2.927
1000	49.83	333.4	−233.2	3.131	2.095	1.465
2000	49.34	335.1	−234.4	1.550	1.053	$7.364\ 10^{-4}$
4000	47.46	341.6	−239.0	$7.455\ 10^{-5}$	$5.366\ 10^{-4}$	3.755
8000	41.17	366.0	−257.2	3.233	2.875	2.020
16000	26.84	446.5	−323.4	1.054	1.754	1.270
32000	11.12	663.8	−524.9	$2.184\ 10^{-6}$	1.303	1.031

$$\left.\begin{aligned} c_1&=U+2\sqrt{-\frac{a}{3}}\cos\left(\frac{\epsilon}{3}+\frac{4}{3}\pi\right)\approx U\\ c_2&=U+2\sqrt{-\frac{a}{3}}\cos\frac{\epsilon}{3}\qquad\approx U+\sqrt{gH}\\ c_3&=U+2\sqrt{-\frac{a}{3}}\cos\left(\frac{\epsilon}{3}+\frac{2}{3}\pi\right)\approx U-\sqrt{gH}\end{aligned}\right\}\qquad(3.3)$$

where $\epsilon=\tan^{-1}[(-4a^3/27b^2)-1]^{1/2}$, $a=-(f^2/\nu^2)-gH$, $b=-f^2U/\nu^2$ and c_1, c_2, and c_3 are defined to denote the phase velocity of a meteorological wave, an eastward-moving inertia-gravitational (external) wave, and a westward-moving one, respectively. Table 3.1 shows c_i and νc_i with $U=50$ m.sec.$^{-1}$, f taken at 45°latitude, and $gH=8\times10^4$m.^{2}sec.$^{-2}$.

With the use of (3.2), (3.1) is rewritten as follows:

$$\left.\begin{aligned}&\frac{\partial h_i}{\partial t}+i\nu Uh_i=-i\nu(c_i-U)h_i\\ &h=\sum_{i=1}^{3}h_i\end{aligned}\right\}\qquad(3.4)$$

where h_i stands for any perturbation quantity (u_i, v_i, or ϕ_i), and the subscript i corresponds to those of (3.3). It is seen that the form of (3.4) is identical with (2.1) of the previous section. (3.1) can also be written in the following symbolic form, which will be used hereafter for the sake of convenience,

$$\frac{\partial h}{\partial t}=F_1+F_2\qquad(3.5)$$

where

$$F_1=-U\partial h/\partial x$$

F_2=the right-hand side of (3.1).

The problem is, now, to do the time integration of (3.5) with various methods and to examine their characteristics. The names of the methods in the following should correspond to those in section 2.

Method A.—Time integration of (3.5) takes the form

$$h^{\tau+1}-h^{\tau}=\Delta t\cdot F_1^{\tau+1}+\Delta t\cdot F_2^{\tau+1}\qquad(3.6)$$

where τ, $\tau+1$, and Δt are two time-levels and the interval between them respectively. $F_{1,2}^{\tau+1}$ means that $F_{1,2}$ should be evaluated by using $h^{\tau+1}$. In this case (3.4) becomes

$$h_i^{\tau+1}-h_i^{\tau}=-i\nu c_i(\Delta t)h_i^{\tau+1}.\qquad(3.7)$$

This is the same as (2.3) with $\alpha=\nu c_i(\Delta t)$. The amplification rate of h_i, i.e., R_1, and a measure of the fictitious change of phase velocity[1] are shown in figure 3.1 against the parameter $b=\nu c_i(\Delta t)$. From this figure and table 3.1, it is easy to see that for a specified wavelength and Δt, damping of the wave is highly selective for gravitational waves, for which νc_i is several times larger than for a low-frequency wave. This is the merit of this method. It should be noted, however, that damping of the meteorological wave is also unavoidable, however small Δt may be. Consequently, successive use of (3.6) will at last cause a noticeable damping of the low-frequency wave.

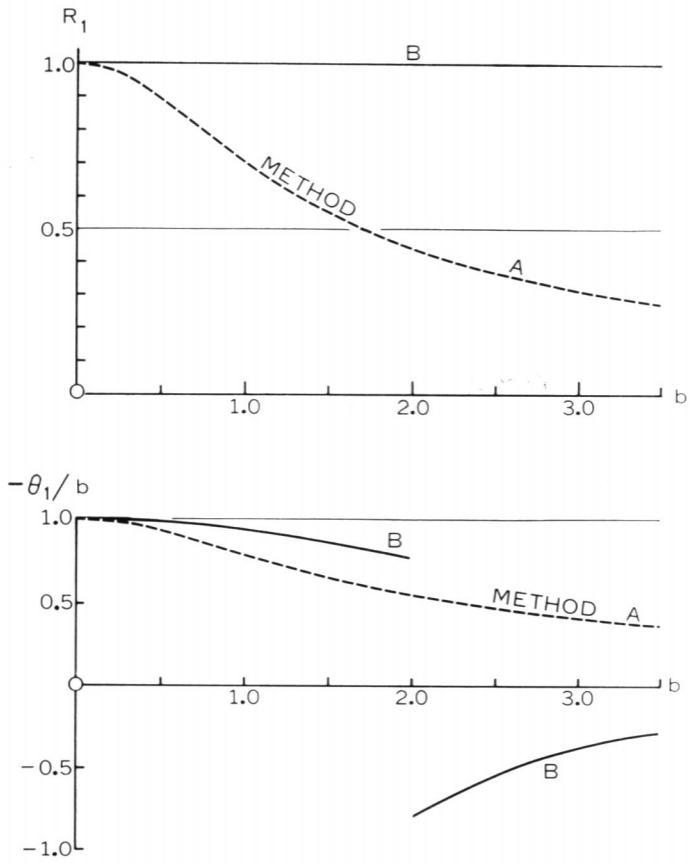

FIGURE 3.1.—The upper figure shows amplification rate of computed physical mode, R_i, as a function of parameter b. $b=\nu c\Delta t$. The lower figure shows the ratio of phase velocity of computed physical mode to the true phase velocity (c) as a function of b. For example, suppose $b=\nu c\Delta t=1.5$. Then, if we use Method A, an amplitude of computed wave at a time level $\tau+1$ is 0.55 times that at τ, and a wave moves with a speed $0.66\times c$. If we use Method B, an amplitude of wave does not change and a moving speed of computed wave is $0.86\times c$.

[1] As mentioned before, the amplification rate and phase velocity of the computed mode are given by R_1 and $-\vartheta_1/\nu(\Delta t)$ respectively, where R_1 and ϑ_1 are the magnitude and phase angle of the eigenvalue for an amplification matrix of (3.7). Accordingly, $-\vartheta_1/\nu c_i(\Delta t)=-\vartheta_1/b$ is the ratio of phase velocity of the computed value to the true phase velocity.

As for the error in phase velocity, it is large when b is large.

Method B.—Time integration of (3.5) takes the form

$$h^{\tau+1}-h^{\tau}=\frac{\Delta t}{2}(F_1^{\tau+1}+F_1^{\tau})+\frac{\Delta t}{2}(F_2^{\tau+1}+F_2^{\tau}). \tag{3.8}$$

The form of (3.4) corresponding to (3.8) is

$$h_i^{\tau+1}-h_i^{\tau}=-i\,\frac{\nu c_i(\Delta t)}{2}\,h_i^{\tau+1}-i\,\frac{\nu c_i(\Delta t)}{2}\,h_i^{\tau} \tag{3.9}$$

which is equivalent to (2.4) with $\alpha=\nu c_i(\Delta t)/2=b/2$. In this case, too, the amplification rate and ratio of the phase velocity of the computed h_i to the true one are estimated and are shown in figure 3.1. This method is neutral for any value of b. Therefore, amplitudes of both meteorological and gravitational waves are to be conserved, although very small amplification or damping of waves may be inevitable in practice because of round-off error in the numerical computation and some error in obtaining $h^{\tau+1}$ as a solution of (3.8). As for the error in phase velocity, those of gravitational waves are much larger than that of the meteorological wave. As a consequence, it may be concluded that, if we are not concerned with predicted phases of gravitational waves, we can make a time step in (3.8) somewhat larger than what is usually required in the explicit integration of the primitive equations. It seems desirable for users of this method to apply it after gravitational waves are mostly filtered by other methods (such as method A or filtering initialization). This is particularly important when a system of nonlinear equations is treated, where the three waves are no longer independent of each other.

Method C.—Tseng Ch'ing-ts'un [12] formulated a scheme of time integration of the primitive equation in which the linear terms of the equations were written with average values at two time-levels and the nonlinear term and β-term were to be evaluated explicitly by using values only at the time-level τ. His method was used with some changes by Bortnikov [1], with a grid size of 300 km. and time increment of 3 hr., which is very large compared to the ratio of space increment to phase velocity of gravitational waves. It should be noted that a spatial smoothing was made of some terms at each step.

Applying Tseng's idea to (3.5) we have

$$h^{\tau+1}-h^{\tau}=\Delta t\cdot F_1^{\tau}+\frac{\Delta t}{2}(F_2^{\tau+1}+F_2^{\tau}). \tag{3.10}$$

Hence a corresponding formula for each wave is derived,

$$\begin{aligned}h_i^{\tau+1}-h_i^{\tau}&=-i\nu U(\Delta t)h_i^{\tau}-i\nu(c_i-U)\,\frac{\Delta t}{2}\,(h_i^{\tau+1}+h_i^{\tau})\\&=-i\nu\,\frac{(c_i-U)}{2}\,(\Delta t)h_i^{\tau+1}-i\nu\left(U+\frac{c_i-U}{2}\right)(\Delta t)h_i^{\tau}\end{aligned} \tag{3.11}$$

This is equivalent to Method C in section 2. From (2.2) and (3.11) it follows that

$$\left.\begin{aligned}\alpha&=\nu\,\frac{c_i-U}{2}\cdot\Delta t\\ \beta&=\nu\,\frac{c_i+U}{2}\cdot\Delta t\end{aligned}\right\}. \tag{3.12}$$

For the meteorological wave and one of the two gravitational waves, $|\beta|$ becomes larger than $|\alpha|$, and $|\beta|<|\alpha|$ holds only for the other gravitational wave. Accordingly, the discussion in the previous section suggests that the former two waves will be amplified while damping is to be expected for only one wave.

If we also use finite difference representation for space differentiation in the beginning parts of this section, (3.1) through (3.5) are modified to some extent. Some considerations concerning these are given in Appendix 1. In order to discuss fairly Tseng's method we should use these modified forms. As a result we will have different forms of α and β in (3.12). However, the modifications of α and β may be small except for short waves with the wavelength of several grids. Such a scheme is not really computationally stable. This instability cannot be eliminated by reducing a time interval.

Method 1.—The centered time difference scheme is the one most widely used at present. Its form and corresponding formula for each mode of waves are,

$$h^{\tau+1}-h^{\tau-1}=2\cdot\Delta t(F_1^{\tau}+F_2^{\tau}) \tag{3.13}$$

$$h_i^{\tau+1}-h_i^{\tau-1}=-i2\nu c_i(\Delta t)h_i^{\tau} \tag{3.14}$$

respectively. Some characteristics of this method are illustrated in figure 4.1. In case of (3.14), a parameter b in the figure is equal to $|\nu c_i(\Delta t)|$. Computational stability requires that $|\nu c_i(\Delta t)|<1$. With the use of typical value of νc_i in table 3.1, the maximum allowable value of Δt is estimated and listed in table 3.2 as a function of the shortest wavelength to be treated. When one uses a functional form in representing the distribution of quantities and deduces F_1 and F_2 in (3.13) by analytical computations, e.g., the use of Fourier series or a spherical harmonics expansion method, then Δt should be determined by the smallest scale one treats. Or, alternatively, if the time interval is fixed to some value, all

TABLE 3.2—*The shortest wavelength to be treated (L) and maximum value of the time increment (Δt) which satisfies the computational stability condition for Method 1. It is assumed that a wave is treated analytically, i.e., a spectrum method is used.*

L (km.)	Δt (sec.)
250	119
500	239
1000	477
2000	950
4000	1864

waves shorter than a critical wavelength should be truncated from the functional form.

The most troublesome deficiency in this method is the occurrence of the computational mode. If the amplitude of this mode becomes large it is meaningless to continue the time integration.

Method D.—This method is written as follows:

$$h^{\tau+1}-h^{\tau-1}=2\cdot\Delta t F_1^{\tau}+2\cdot\Delta t F_2^{\tau+1} \tag{3.15}$$

Namely, the advection term is estimated explicitly and the other terms implicitly. The corresponding formula for each mode is

$$h_i^{\tau+1}-h_i^{\tau-1}=-2i\nu(c_i-U)\cdot(\Delta t)h_i^{\tau+1}-2i\nu U\cdot(\Delta t)h_i^{\tau} \tag{3.16}$$

This is identical with (2.6) if we put

$$\begin{aligned}\alpha&=2\nu(c_i-U)\cdot(\Delta t)\\ \beta&=2\nu U\cdot(\Delta t)\end{aligned} \tag{3.17}$$

If we suppose $c_i=U$ in (3.16), it takes the form of (3.14). If we neglect the second term on the right hand side of (3.16), assuming that $|c_i|\gg U$, then we have a form similar to (3.7). Hence this method looks favorable from the viewpoint of effective damping of gravitational waves. Strictly speaking, however, this method is not computationally stable. This will be explained as follows. The conclusion from the previous section was that the condition of computational stability of (3.16) is $|\alpha|>|\beta|$. In the case of a meteorological wave, α takes a small and non-zero value and this condition cannot be satisfied. On the other hand for gravitational waves, $|\alpha|$ is much larger than $|\beta|$, and those waves will be damped. Consequently, this marching scheme cannot be used for a long-range time integration.

However, since the amplification rate of the meteorological wave is very small, this method may be used in short-range integrations. A test computation of this kind was attempted by using a simple linearized model. The model adopted is the same as (3.1), $U=50$ m.sec.$^{-1}$, f is taken at 45° latitude, and $gH=8\times10^4$ m.^{2}sec.$^{-2}$. The wavelength of the sinusoidal wave we treated is 4500 km. To give the initial values of u, v, and ϕ, $S_1=1000$ gpm., $S_2=50$ gpm. and $S_3=50$ gpm. were taken in (3.2). Then, computations were repeated with $\Delta t=1$ hr. by the scheme (3.15), were h stands for u, v, and ϕ. In computing $\phi^{\tau+1}$, we made a slight change in the scheme. Namely, v^{τ} was used instead of $v^{\tau+1}$ for evaluating the first term on the right hand side of the third equation of (3.1). Then substituting $u^{\tau+1}$ in the third equation from the first equation, in which $v^{\tau+1}$ was substituted from the second equation, a one-dimensional Helmholtz-type equation for $\phi^{\tau+1}$ was obtained. In our test, a finite difference computation with a 300 km. grid was used and a Helmholtz-type equation was solved by matrix inversion. With the solution of $\phi^{\tau+1}$, both $u^{\tau+1}$ and $v^{\tau+1}$ were easily computed. In this way calculations were continued up to five days, i.e., 120 time steps. In figure 3.2 the values of ϕ and $\partial u/\partial x$ at $x=0$ are plotted together with the true variations. Effective damping of gravitational waves is clearly seen. Changes in amplitude of the meteorological wave are negligible so far as this example is concerned. A rough estimate for our test case shows that the amplification rates for the meteorological wave is $1+O(10^{-3})$ and those for gravitational waves are 0.6 or thereabout.

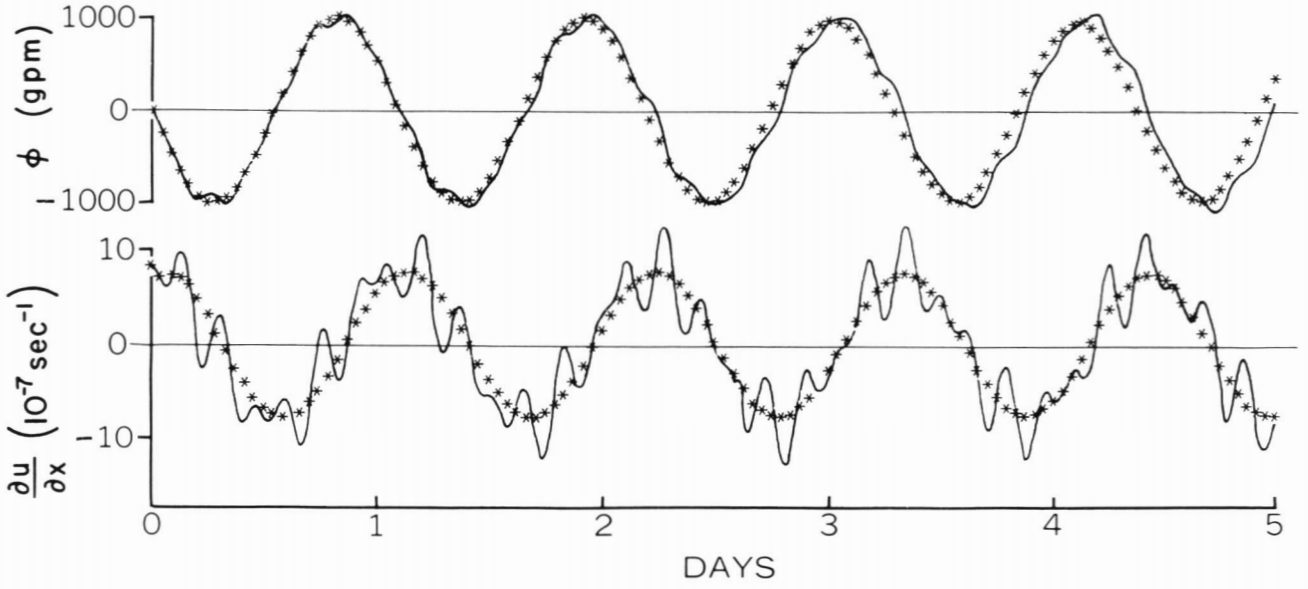

FIGURE 3.2.—Prediction of ø and $\partial u/\partial x$ with a system of equations (3.1). Method D was used with $\Delta t=1$ hr. Time variation of ϕ and $\partial u/\partial x$ at $x=0$ is shown (true value is shown by continuous line and computed value by asterisks).

4. ITERATIVE METHOD

To adopt an implicit scheme in the time integration of (3.1) requires solving some equations involving values at a time-level in advance. In order to avoid this process, we can use some guess in evaluating implicit terms in the equation. This idea makes a computation scheme effectively explicit and similar to the so-called predictor-corrector method.

We shall again write (3.1) in the symbolic form: $\partial h/\partial t=F$, where F is equal to the right hand side of (3.5). $\partial h_i/\partial t=-ivc_ih_i(i=1,2,3)$ is an equation for any component wave which moves independently of the other two waves. This is equivalent to (3.4). Then, it is not difficult to obtain a formula in which $h_i^{\tau+1}$ is written explicitly in terms of h_i^{τ} and $h_i^{\tau-1}$, for each scheme of iteration. In the following the computation scheme written in symbolic form and the corresponding formula for a component wave are given for four methods (where h^* is a value to be estimated at the first step and h^{**}, if necessary, is at the second; F^* and F^{**} show values of F which are evaluated by using h^* and h^{**}, respectively; by definition, b is equal to $\nu c_i(\Delta t)$):

Method 2—(Euler-backward iteration):

$$\begin{cases} h^*-h^{\tau}=\Delta t\cdot F^{\tau} & \text{(Euler method)} \\ h^{\tau+1}-h^{\tau}=\Delta t\cdot F^* & \text{(backward correction)} \end{cases} \tag{4.1}$$

$$h_i^{\tau+1}=(1-\sqrt{-1}b-b^2)h_i^{\tau} \tag{4.2}$$

Method 3—(Modified Euler-backward iteration):

$$\left.\begin{cases} h^*-h^{\tau}=\dfrac{\Delta t}{2}\cdot F^{\tau} \\ h^{**}-h^{\tau}=\Delta t\cdot F^* \end{cases}\right\} \quad \text{(modified Euler method)}$$

$$h^{\tau+1}-h^{\tau}=\Delta t\cdot F^{**} \quad \text{(backward correction)} \tag{4.3}$$

$$h_i^{\tau+1}=\left(1-\sqrt{-1}b-b^2+\sqrt{-1}\,\frac{b^3}{2}\right)h_i^{\tau} \tag{4.4}$$

Method 4—(leapfrog-trapezoidal iteration):

$$\begin{cases} h^*-h^{\tau-1}=2\cdot\Delta t F^{\tau} & \text{(leapfrog method)} \\ h^{\tau+1}-h^{\tau}=\Delta t\cdot\frac{1}{2}(F^*+F^{\tau}) & \text{(trapezodial correction)} \end{cases} \tag{4.5}$$

$$h_i^{\tau+1}=\left(1-b^2-\sqrt{-1}\,\frac{b}{2}\right)h_i^{\tau}-\sqrt{-1}\,\frac{b}{2}\,h_i^{\tau-1} \tag{4.6}$$

Method 5—(leapfrog-backward iteration):

$$\begin{cases} h^*-h^{\tau-1}=2\cdot\Delta t F^{\tau} & \text{(leapfrog method)} \\ h^{\tau+1}-h^{\tau}=\Delta t\cdot F^* & \text{(backward correction)} \end{cases} \tag{4.7}$$

$$h_i^{\tau+1}=(1-2b^2)h_i^{\tau}-\sqrt{-1}bh_i^{\tau-1} \tag{4.8}$$

The characteristic qualities of each method are revealed by the eigenvalues of the amplification matrices for (4.2), (4.4), (4.6), and (4.8). In the case of methods 2 and 3, there exists only one computed mode for each of the three component waves, i.e., the computed physical mode which will be denoted by suffix 1 hereafter. While with methods 4 and 5 we have another mode, i.e., the computational mode to be identified by suffix 2. From the eigenvalues, estimates are made of the amplification rate of each mode and the ratio of phase velocity of the computed mode to the phase velocity to be derived from a parameter b. The latter one is equal to the analytical solution (3.3), if computation of F is made analytically with respect to space. If F is estimated by centered space difference methods b is equal to $\nu c_i'(\Delta t)$ where c_i' is a phase velocity modified due to taking finite differences with respect to space. The ratio of c_i' to c_i is given together with $\nu c_i'$ in Appendix 1 for some cases. Hence, if finite difference methods are used for both space and time, $(-\vartheta/b)\times(c_i'/c_i)$ will yield the ratio of the phase velocity of the computed value to the true phase velocity. Figure 4.1 shows how R_1, R_2, $-\vartheta_1/b$, and $-\vartheta_2/b$ or $-(\vartheta_2+\pi)/b$ depend on b. It is suggested by figure 4.1 and tables A.1 and A.2 in Appendix 1 that a fictitious acceleration of the physical mode by Methods 1, 2, 3, and 5 might be compensated or even overcompensated by a fictitious retardation of the wave as a result of finite differencing in space.

The condition for computational stability is $|b|<1.0$ for Method 2, $|b|<\sqrt{2}$ for Methods 3 and 4, and $|b|<$ about 0.8 for Method 5. Consequently, comparing with the criterion for Method 1, we cannot get time economy in computation since iterations are required. If $b=\nu c_i\cdot(\Delta t)$, i.e., when F is computed analytically, the above criterion gives a relation between Δt and the shortest wavelength we can treat, as shown already in table 3.2. When an estimate of F is made by centered space differences, i.e., in the case of $b=\nu c_i'\cdot(\Delta t)$, the maximum value of $\nu c_i'$, which is usually a function of grid size and also depends on the finite difference scheme, determines the maximum time interval. For example, consider the case given in Appendix 1 and assume that $|\nu c_i'\cdot(\Delta t)|<1$ is a stability condition. Then, the maximum tolerable value of Δt for a grid size of 250 km. is 740 sec. or 560 sec., depending on whether the three-point method or five-point method is used in estimating the horizontal gradient of a scalar field quantity. It is 1470 sec. or 1110 sec. for a 500-km. grid and 2820 sec. or 2170 sec. for a 1000-km. grid.

Figure 4.1 shows that the selective damping for gravitational waves can be made the largest by Method 3. It is characteristic of Methods 4 and 5 that they result in a high rate of damping of the computational mode, especially that corresponding to the meteorological wave. Only Method 1 is neutral, provided the stability condition is satisfied. Consequently, it seems a good design to use Method 1 at most time steps but to utilize some kind of

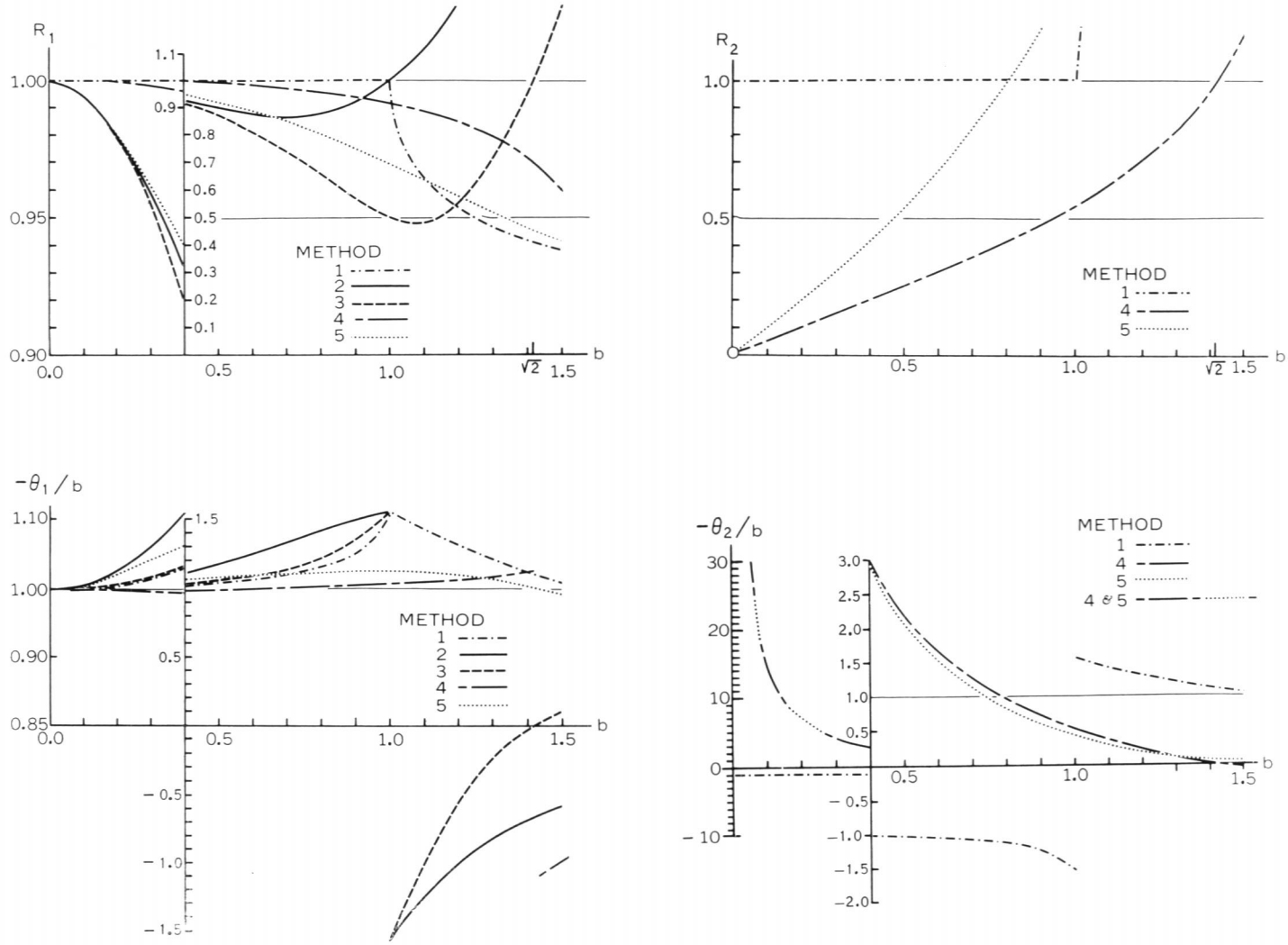

FIGURE 4.1.—Amplification rate of computed physical mode (the upper left figure) and that of computational mode (the upper right figure) are shown against parameter b. $b=\nu c\Delta t$, if a spectrum method is used in treating a wave. When a centered difference grid method is used, $b=\nu c'\Delta t$. (νc and $\nu c'$ are listed in tables 3.1, A.1, and A.2.) The lower left figure shows ratio of phase velocity of computed physical mode to c (or c', if the grid method is used). Ratio of phase velocity of computational mode to c (or c') is shown in the lower right figure. In three figures, vertical scale is changed at $b=0.4$. Suppose that $b=0.5$ and Method 4 is used. Then, an amplitude of computed physical mode at a time level $\tau+1$ is 0.99 times that at τ. It moves with a speed $0.99\times c$, if a spectrum method is used, or with a speed $0.99\times c'$, if a centered difference grid method is used. An amplitude of computational mode at $\tau+1$ is 0.25 times that at τ. Its moving speed is $2.15\times c$ or $2.15\times c'$.

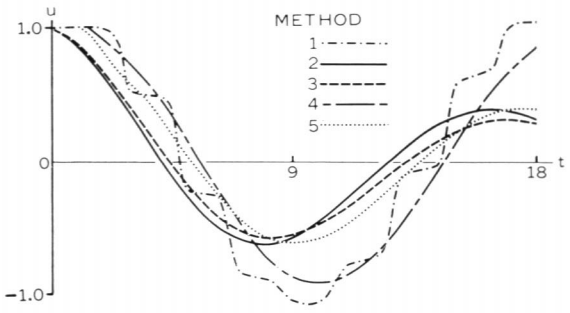

FIGURE 4.2.—Prediction of inertia oscillation by iterative methods, with $\Delta t=1$ hr. u is plotted. $u^1=u^0=1$ was assumed for Methods 1, 4, and 5.

iterative methods intermittently. In doing so, the selection and combination of appropriate iterative methods has to be based upon their particular properties. To use an iterative scheme at every step may not be suitable for some purposes, since the effect of damping of the wave will accumulate with time. For example, let us assume a wave of length 4000 km. and phase velocity 15 m. sec.$^{-1}$ Then $\Delta t=20$ min. makes b approximately 0.028. The amplification rate of Method 2 for this value of b is 0.99961. Therefore, with the exclusive use of Method 2, an amplitude of the wave will be decreased by 2.8 percent in one day (72 steps), resulting in the decrease of kinetic energy of disturbance by 5.5 percent.

As a test of the iterative methods, the differential equation governing inertia oscillation was integrated

TABLE 5.1.—*Summary of the properties of the methods studied. In "difference equation", F_1 and F_2 represent nonlinear and linear terms, respectively, and $F=F_1+F_2$. "Number of time levels" means what is associated with each marching step. In "computational stability", $b=vc\Delta t$ if a spectrum method is used in treating a wave. $b=vc'\Delta t$, if a centered difference grid method is used. In "physical mode", retardation or acceleration means a fictitious change of phase velocity resulted only from finite differencing in time.*

	Method	Difference Equation	Number Of Time Levels	Computational Stability	Physical Mode		Computational Mode
					Amplitude	Phase	Amplitude
IMPLICIT	A backward	$h^{\tau+1}-h^{\tau}=\Delta t F^{\tau+1}$	2	Absolutely stable	Highly selective damping	Retardation	None
	B trapezoidal	$h^{\tau+1}-h^{\tau-1}=\frac{\Delta t}{2}(F^{\tau+1}+F^{\tau})$	2	Absolutely stable	No change	Little retardation	None
	C partly	$h^{\tau+1}-h^{\tau}=\Delta t F_1{}^{\tau}+\frac{\Delta t}{2}(F_2{}^{\tau+1}+F_2{}^{\tau})$	2	Unstable for meteorological wave and one gravity wave			None
	D partly	$h^{\tau+1}-h^{\tau}=2\Delta t F_1{}^{\tau}+2\Delta t F_2{}^{\tau+1}$	3	(Very weak) unstable for meteorological wave	Damping of gravity wave and weak amplifying of meteorological wave		Damping
EXPLICIT	0 forward	$h^{\tau+1}-h^{\tau}=\Delta t F^{\tau}$	2	Unstable			None
	1 leapfrog (centered)	$h^{\tau+1}-h^{\tau-1}=2\Delta t F^{\tau}$	3	Conditionally stable ($b<1$)	No change	Moderate acceleration	No change
ITERATIVE	2 Euler-backward	$h^{*}-h^{\tau}=\Delta t F^{\tau}$ $h^{\tau+1}-h^{\tau}=\Delta t F^{*}$	2	Conditionally stable ($b<1$)	Moderately selective damping	Large acceleration	None
	3 modified Euler-backward	$h^{*}-h^{\tau}=\frac{\Delta t}{2}F^{\tau}$ $h^{**}-h^{\tau}=\Delta t F^{*}$ $h^{\tau+1}-h^{\tau}=\Delta t F^{**}$	2	Conditionally stable ($b<\sqrt{2}$)	Highly selective damping	Moderate acceleration	None
	4 leapfrog-trapezoidal	$h^{*}-h^{\tau-1}=2\Delta t F^{\tau}$ $h^{\tau+1}-h^{\tau}=\frac{\Delta t}{2}(F^{*}+F^{\tau})$	3	Conditionally stable ($b<\sqrt{2}$)	Little damping	Little error	Very effective damping (in particular of meteorological wave)
	5 leapfrog-backward	$h^{*}-h^{\tau-1}=2\Delta t F^{\tau}$ $h^{\tau+1}-h^{\tau}=\Delta t F^{*}$	3	Conditionally stable ($b<0.8$)	Moderately selective damping	Moderate acceleration	Damping

The equation, for which the iterative methods were applied, is the same as (2.5). $f=\pi/9$ (hr.$^{-1}$) was assumed. Hence, the period of oscillation is 18 hr. As a starting value, $w^0=u^0=1$ was given for Methods 2 and 3. For Methods 1, 4, and 5, it is also necessary to give the value of w at a time-level nearest to the initial, i.e., w^1 or w^{-1}, to start the calculation. If we estimate w^1 from w^0 by a modified Euler method which we used to start the calculation by Method 1 in figure 2.5, we cannot detect the existence of computational mode. In order to force a large initial amplitude of the computational mode the integrations with Methods 1, 4, and 5 were begun with $w^1=w^0$. Figure 4.2 shows the predictions of u in the case of $\Delta t=1$ hr. For this case we have $b=2\pi\cdot(\Delta t)/(\text{period})=0.35$. On the other hand, the ordinate values against this value of b in figure 4.1 suggest damping of the physical mode of oscillation by Methods 2, 3, and 5, the considerable damping of the computational mode by Method 4 (82 percent at each step) and by Method 5 (63 percent), the conservation of both modes by Method 1, and the fictitious increase of phase velocity by Method 2. It is seen that the features of the curves in figure 4.2 are the same with these suggestions. The predictions made with $\Delta t=2$ hr., for which the corresponding value of b is 0.70, showed the fast damping of the computational mode by Method 4 and slow damping by Method 5. In case of $\Delta t=2.7$ hr., for which $b=0.94$, Method 2 yielded a very slow damping of the physical mode and a large fictitious decrease in period of oscillation; Method 3 rapidly damped the oscillation; Method 4 damped the computational mode; and the computation by Method 5 became unstable. All of these coincide quite well with what we observed in figure 4.1.

5. SUMMARY

The main properties of the methods considered in sections 2 to 4 are shown in table 5.1.

The properties of Method A (two time-levels, backward implicit method), Method B (two time-levels, trapezoidal implicit method), Method C (two time-levels, partly implicit method), and Method 1 (three time-levels, leapfrog method) have been discussed so far, more or less. They are confirmed in section 2, where the characteristics of these methods in case of wave equation in simple form are described. In section 3, we consider these methods especially from the viewpoint of their applicability to the integration of the primitive equations.

Methods A and B are computationally absolutely stable. In the use of these methods, the amount of computation required to solve the non-trivial equations for the quantities at a new time-level and the decrease of accuracy of the predicted low frequency wave should be weighed against the advantage of a long time interval in a marching process. The amplitude of any wave will not be changed with Method B. Method A results in a damping which increases with the increasing value of the parameter b. ($b=vc\Delta t$ if a spectrum method is used in treating a wave. When we use a centered difference grid method, $b=vc'\Delta t$ where c' is a modified phase velocity.) The property of selective damping of wave is useful for

reducing the noise in the solution of the primitive equations.

Method 1 has no damping effect for either physical or computational modes.

The characteristics of Method D (three time-levels partly implicit method) are made clear in sections 2 and 3. It yields an effective damping of gravitational waves. It is because of this that, despite a slight computational instability of this method, we used it in section 3. Method D may be used with a relatively long time interval, say one hour, for the short-range integration of the primitive equation.

The numerical properties of Methods 2, 3, 4, and 5 (iterative methods) are investigated in section 4. The condition of computational stability for Methods 3 and 4 is somewhat weak as compared with Methods 1, 2, and 5. By utilizing the characteristic features of Methods 1, 3, and 4, we may synthesize a scheme more desirable than any of its parts. Namely, after using Method 1, Method 4 is employed for a few steps to eliminate the computational mode, then Method 3 is applied to damp the noise before returning to Method 1, and so on.

APPENDIX 1.—FICTITIOUS CHANGE OF THE PHASE VELOCITY DUE TO THE USE OF CENTERED SPACE DIFFERENCES

If computations are made accurately of an advection term and the right hand side of (3.1), the phase velocities of three waves, c_1, c_2, and c_3, are given by (3.3). We will call these analytical phase velocities.

Let us estimate the horizontal gradient of some quantities, say $z(x)$, by a finite difference calculation. If $z(x)=z_0 \exp[i\nu(x+x_\nu)]$ is assumed, it follows that $\partial z/\partial x=i\nu z$. The corresponding finite difference formula for a usual three-point method is given by

$$\frac{z(x+\Delta)-z(x-\Delta)}{2\Delta}=i\frac{\sin\nu\Delta}{\Delta}z(x),$$

where Δ is the space-increment. The similar one for a five-point method is

$$\frac{8\cdot z(x+\Delta)-8\cdot z(x-\Delta)-z(x+2\Delta)+z(x-2\Delta)}{12\cdot\Delta}=i\frac{(\sin\nu\Delta)\cdot(4-\cos\nu\Delta)}{3\Delta}z(x)$$

The above two finite difference formulas take a common form, namely $\partial z/\partial x\approx i\nu' z$ instead of analytical value $i\nu z$.

Now, with the use of the above expression for a horizontal gradient and an assumption of an equal wave length for u, v, and ϕ, (3.1) is modified as follows:

$$\left.\begin{aligned}\frac{\partial u}{\partial t}+i\nu' Uu&=fv-i\nu'\phi\\ \frac{\partial v}{\partial t}+i\nu' Uv&=-fu\\ \frac{\partial\phi}{\partial t}+i\nu' U\phi&=fUv-i\nu' gHu\end{aligned}\right\}\qquad(3.1\text{–A})$$

The solutions of (3.1–A) are given by

$$\left.\begin{aligned}u&=\sum_{i=1}^{3}u_i, & u_i&=\phi_i\frac{\nu\nu'\left(\frac{\nu'}{\nu}U-c_i'\right)}{f^2-\left(\frac{\nu'}{\nu}U-c_i'\right)^2\nu^2}\\ v&=\sum_{i=1}^{3}v_i, & v_i&=\phi_i\frac{i\nu' f}{f^2-\left(\frac{\nu'}{\nu}U-c_i'\right)^2\nu^2}\\ \phi&=\sum_{i=1}^{3}\phi_i, & \phi_i&=S_i\exp i\nu(p\Delta-c_i't)\end{aligned}\right\}\qquad(3.2\text{–A})$$

where p is the integer and $\nu=2\pi/(n\Delta)$, where n (integer ≥ 2) is a number of grid points within a wavelength, i.e., in other words, $n\Delta$ means wave length. ν' may be written in terms of n and Δ,

$$\nu'=\frac{1}{\Delta}\sin\frac{2\pi}{n}\qquad\text{for the three-point method}$$

$$\nu'=\frac{1}{3\Delta}\sin\frac{2\pi}{n}\left(4-\cos\frac{2\pi}{n}\right)\qquad\text{for the five-point method.}$$

In (3.2–A), $c_i'(i=1, 2, 3)$ are phase velocities of three component waves in a system of linearized equations (3.1–A) and should be obtained as solutions of the equation

$$\left(\frac{\nu'}{\nu}U-c'\right)^3-gH\frac{\nu'^2}{\nu^2}\left(\frac{\nu'}{\nu}U-c'\right)+\frac{f^2}{\nu^2}c'=0.$$

We shall call these phase velocities modified phase velocities. It is seen, from the comparison of the above equation with the corresponding one in section 3, that c' is the same with c in the case where U and gH are modified to $\frac{\nu'}{\nu}U$ and $\left(\frac{\nu'}{\nu}\right)^2 gH$, respectively. As ν'/ν is nearly equal to one for large n, the fictitious change of phase velocities due to space finite differencing is small for relatively long waves. On the contrary, ν'/ν is smaller than about 0.9 for $n\leq 8$ (in the case of the three-point method) or for $n\leq 5$ (five-point method), and an error in the phase velocity of waves corresponding to these n becomes large. An important formula which is derived from (3.1–A) and (3.2–A) and is equivalent to (3.4) is

$$\frac{\partial h_i}{\partial t}+i\nu' Uh_i=-i(\nu c_i'-\nu' U)h_i.\qquad(3.4\text{–A})$$

TABLE A.1.—*Ratio* (c_1'/c_1) *of the modified phase velocity* (c_1') *to the analytical phase velocity* (c_i) *and* $\nu c_i'$, *in case of a three-point finite difference scheme with a grid size of 250, 500, and 1000 km. n is the number of grid points within a wavelength, i.e.,* $n\times$(*grid size*)=*wavelength. Assumed values of U, gH, f are the same as those shown in table 3.1.*

n	c_1'/c_1 (%)	c_2'/c_2 (%)	c_3'/c_3 (%)	$\nu c_1'$ (sec.$^{-1}$)	$\nu c_2'$ (sec.$^{-1}$)	$\lvert\nu c_3'\rvert$ (sec.$^{-1}$)
250-km. grid						
2	0.0	2.5	3.5	--------	$1.028\ 10^{-4}$	$1.028\ 10^{-4}$
3	41.0	41.5	41.5	$1.713\ 10^{-4}$	$1.159\ 10^{-3}$	8.110
4	63.4	63.8	63.8	1.984	1.337	9.352
5	75.4	75.8	75.8	1.885	1.272	8.898
6	82.4	82.8	82.8	1.713	1.159	8.110
7	86.8	87.2	87.2	1.543	1.048	7.331
8	89.8	90.2	90.2	1.391	$9.492\ 10^{-4}$	6.640
9	91.8	92.2	92.2	1.260	8.643	6.046
10	93.3	93.7	93.7	1.148	7.918	5.540
20	98.1	98.5	98.5	$5.688\ 10^{-5}$	4.287	3.001
40	99.4	99.7	99.7	2.338	2.398	1.698
500-km. grid						
2	0.0	4.9	7.0	--------	$1.028\ 10^{-4}$	$1.028\ 10^{-4}$
3	39.3	42.1	42.1	$8.295\ 10^{-5}$	5.890	4.121
4	62.5	64.3	64.3	9.680	6.766	4.734
5	74.5	76.3	76.3	9.175	6.445	4.510
6	81.6	83.3	83.3	8.295	5.890	4.121
7	86.0	87.6	87.7	7.417	5.342	3.739
8	89.0	90.6	90.6	6.633	4.859	3.400
9	91.0	92.6	92.6	5.952	4.445	3.112
10	92.5	94.1	94.1	5.365	4.094	2.867
20	97.5	98.8	98.8	2.294	2.376	1.678
40	99.1	99.8	99.9	$6.615\ 10^{-}$	1.556	1.153
1000-km. grid						
2	0.0	9.8	14.0	--------	$1.028\ 10^{-4}$	$1.028\ 10^{-4}$
3	36.2	44.1	44.3	$3.681\ 10^{-5}$	3.122	2.191
4	59.2	65.9	66.0	4.416	3.538	2.480
5	71.6	77.8	77.9	4.149	3.385	2.374
6	78.8	84.7	84.8	3.681	3.122	2.191
7	83.4	89.0	89.1	3.213	2.864	2.012
8	86.5	91.8	92.0	2.795	2.639	1.857
9	88.7	93.7	93.9	2.434	2.448	1.727
10	90.3	95.1	95.3	2.124	2.288	1.619
20	96.5	99.2	99.4	$6.439\ 10^{-6}$	1.547	1.148

TABLE A.2.—*Ratio* (c'_i/c_i) *of the modified phase velocity* (c'_i) *to the analytical phase velocity* (c_i) *and* $\nu c'_i$, *in the case of a five-point finite difference scheme with a grid size of 250, 500, and 1000 km. Refer to table A.1 for further explanation.*

n	c_1'/c_1 (%)	c_2'/c_2 (%)	c_3'/c_3 (%)	$\nu c_1'$ (sec.$^{-1}$)	$\nu c_2'$ (sec.$^{-1}$)	$\lvert\nu c_3'\rvert$ (sec.$^{-1}$)
250-km. grid						
2	0.0	2.5	3.5	--------	$1.028\ 10^{-4}$	$1.028\ 10^{-4}$
3	61.8	62.1	62.1	$2.585\ 10^{-4}$	$1.734\ 10^{-3}$	$1.213\ 10^{-3}$
4	84.4	84.9	84.9	2.654	1.779	1.245
5	93.0	93.2	93.2	2.326	1.563	1.093
6	96.4	96.5	96.5	2.005	1.351	$9.448\ 10^{-4}$
7	98.0	98.1	98.1	1.741	1.178	8.239
8	98.8	98.8	98.8	1.531	1.040	7.278
9	99.2	99.3	99.3	1.362	$9.304\ 10^{-4}$	6.509
10	99.5	99.5	99.5	1.225	8.411	5.884
20	100.0	100.0	100.0	$5.796\ 10^{-5}$	4.351	3.046
40	100.0	100.0	100.0	2.352	2.406	1.698
500-km, grid						
2	0.0	4.9	7.0	--------	$1.028\ 10^{-4}$	$1.028\ 10^{-4}$
3	61.3	62.4	62.4	$1.274\ 10^{-4}$	8.732	6.109
4	84.4	85.1	85.1	1.309	8.958	6.267
5	92.8	93.3	93.3	1.143	7.882	5.515
6	96.3	96.6	96.6	$9.787\ 10^{-5}$	6.833	4.781
7	97.9	98.1	98.1	8.439	5.981	4.185
8	98.7	98.9	98.9	7.358	5.306	3.713
9	99.2	99.3	99.3	6.483	4.767	3.337
10	99.4	99.5	99.5	5.764	4.333	3.033
20	100.0	100.0	100.0	2.351	2.405	1.698
40	100.0	100.0	100.0	$6.674\ 10^{-6}$	1.559	1.155
1000-km grid						
2	0.0	9.8	14.0	--------	$1.028\ 10^{-4}$	$1.028\ 10^{-4}$
3	59.3	63.4	63.5	$6.023\ 10^{-5}$	4.488	3.142
4	83.2	85.7	85.7	6.205	4.598	3.219
5	92.0	93.7	93.7	5.335	4.076	2.855
6	95.7	96.9	96.9	4.472	3.571	2.503
7	97.5	98.3	98.3	3.758	3.165	2.220
8	98.4	99.0	99.0	3.182	2.846	2.000
9	98.9	99.4	99.4	2.716	2.596	1.828
10	99.3	99.6	99.6	2.335	2.397	1.692
20	99.9	100.0	100.0	$6.669\ 10^{-6}$	1.559	1.155

The ratio of modified phase velocity to an analytical one for some specified cases is shown in tables A.1 and A.2. $\nu c_i'$ is a useful parameter for examining properties of a time integration scheme of (3.1-A). These values are listed in the same tables also.

APPENDIX 2.—SOLUTIONS OF $\lambda^2+(A+Bi)\lambda+(C+Di)=0$

In sections 2 and 4 we had to solve the above type equation frequently. A, B, C, and D are real values and $i=\sqrt{-1}$. The two solutions are given by

$$\lambda_1=\left(-\frac{A}{2}+\frac{1}{2\sqrt{2}}(R+\sqrt{R^2+I^2})^{1/2}\right)+\left(-\frac{B}{2}+\frac{1}{2\sqrt{2}}\frac{I}{(R+\sqrt{R^2+I^2})^{1/2}}\right)i$$

$$\lambda_2=\left(-\frac{A}{2}-\frac{1}{2\sqrt{2}}(R+\sqrt{R^2+I^2})^{1/2}\right)+\left(-\frac{B}{2}-\frac{1}{2\sqrt{2}}\frac{I}{(R+\sqrt{R^2+I^2})^{1/2}}\right)i$$

where

$$R=A^2-B^2-4C$$

$$I=2AB-4D.$$

ACKNOWLEDGMENTS

The author wishes to express his thanks to Drs. J. Smagorinsky, S. Manabe, and K. Bryan who have given him encouragement throughout this study. Particularly, J. Smagorinsky read the manuscript very carefully. He wishes to thank also Mrs. J. Snyder, Mrs. R. Brittain, and Mr. E. Rayfield for the assistance he has received in preparing this paper.

REFERENCES

1. S. A. Bortnikov, "Experience With Short Range Weather Prediction on the Basis of the Solution of a Complete System of Thermohydrodynamic Equations," [Opyt kratkosrochnogo prognoza pogody na osnove reshenīâ poleĭ sistemy uravneniĭ termogidrodinamiki] *Meteorologiâ i Gidrologiâ*, Moscow, No. 11, 1962, pp. 12–19. (Translated by I. A. Donehoo, U.S. Weather Bureau, 1963).
2. A. Eliassen, "On Numerical Integration of Certain Partia Differential Equations by Means of the 'Improved Euler-Cauchy Method' ", *Technical Note* No. 1, Institute of Theoretical Meteorology, University of Oslo, 1963.
3. A. Grammeltvedt, "A Numerical Integration Experiment Using the Primitive Equations for a Two-Layer Model of the Atmosphere," *Technical Note* No. 3, Institute of Theoretical Meteorology, University of Oslo, 1963.
4. K. Hinkelmann, "Der Mechanismus des Meteorologischen Lärmes," *Tellus*, vol. 3, No. 4, Nov. 1951, pp. 285–296.
5. D. K. Lilly, "On the Computational Stability of Numerical Solutions of Time Dependent Non-Linear Geophysical Fluid Dynamics Problems," *Monthly Weather Review*, vol. 93, No. 1, January 1965, pp. 11–26.
6. K. Miyakoda, "The Methods of Numerical Time Integration

of One-Dimensional Linear Equations and Their Inherited Errors," *Journal of the Meteorological Society of Japan*, Ser. 2, vol. 38, No. 6, Dec. 1960, pp. 259–287.

7. N. A. Phillips, "On the Problem of Initial Data for the Primitive Equations," *Tellus*, vol. 12, No. 2, May 1960, pp. 121–126.
8. N. A. Phillips, "An Example of Non-Linear Computational Instability," pp. 501–504 in *The Atmosphere and the Sea in Motion*, Rockefeller Institute Press in association with Oxford University Press, New York, 1959.
9. N. A. Phillips, "Numerical Integration of the Hydrostatic System of Equations With a Modified Version of the Eliassen Finite-Difference Grid," *Proceedings of the International Symposium on Numerical Weather Prediction, Tokyo, 1960*, Meteorological Society of Japan, 1962, pp. 109–120.
10. R. D. Richtmyer, "A Survey of Difference Methods for Non-Steady Fluid Dynamics," *NCAR Technical Notes* 63–,2 NCAR, Boulder 1963, 20 pp.
11. N. G. Turîanskaîa, "Investigation on a Prognostic Method With Implicit Finite Differences," [Issledovanie Prognosticheskoĭ Schemy S Neîavnymi Konechnymi Raznostîami] *Trudy*, Tsentral'nyi Institut Prognozov, Moscow, vyp. 102, 1962, pp. 47–52. (Translated by H. K. Gold, U.S. Weather Bureau, 1963)
12. Tseng Ch'ing-ts'un, "Primenenie polnoĭ sistemy uravneniĭ termogidrodinamikĭ k kratkosrochnomu prognozu pogody v dvukhurovennoĭ modeli," [The Application of an Entire System of Thermohydrodynamic Equations to Short Range Weather Prediction in a Two-Level Model], *Doklady* Akademiĭ Nauk SSSR, vol. 137, No. 1, Mar, 1961, pp. 76–78.
13. S. Uusitalo, "The Numerical Calculation of Wind Effect on Sea Level Elevations," *Tellus*, vol. 12, No. 4, Nov. 1960, pp. 427–435.
14. G. Veronis, "An Analysis of Wind-Driven Ocean Circulation With a Limited Number of Fourier Components," *Journal of Atmospheric Sciences*, vol. 20, No. 6, Nov. 1963, pp. 577–593.

[*Received June 23, 1964; revised November 19, 1964*]

Publications By Weather Bureau Authors

J. K. Angell, "Some Velocity and Momentum Flux Statistics Derived from Transosonde Flights," *Quarterly Journal of the Royal Meteorological Society*, vol. 90, No. 386, Oct. 1964, pp. 472–477.

J. K. Angell and J. Korshover, "Quasi-Biennial Variations in Temperature, Total Ozone, and Tropopause Height," *Journal of the Atmospheric Sciences*, vol. 21, No. 5, Sept. 1964, pp. 479-492.

M. L. Blanc (with L. P. Smith), "International Agricultural Meteorology," *Agricultural Meteorology*, vol. 1, No. 1, Mar. 1964, pp. 3–13.

H. R. Glahn and J. O. Ellis, "Note on the Determination of Probability Estimates," *Journal of Applied Meteorology*, vol. 3, No. 5, Oct. 1964, pp. 647–650.

A. V. Hardy, "Low Temperature Probabilities in North Carolina," *Bulletin 423*, Agricultural Experiment Station, University of North Carolina, Raleigh, Sept. 1964.

A. J. Kish, "South Carolina Growing Degree Days," *Agricultural Weather Research Series* No. 3, South Carolina Agricultural Experiment Station, Clemson University, Oct. 1964, 28 pp.

R. J. List, K. Telegadas, and G. J. Ferber, "Meteorological Evaluation of the Sources of Iodine 131 Contamination in Pasteurized Milk," *Science*, vol. 146, No. 3640, Oct. 2, 1964, pp. 59–64.

M. D. Magnuson, "Accidents and Deaths from Weather Extremes," pp. 519-532 of *Medical Climatology*, Sidney Licht, Ed., E. Licht Publisher, New Haven, 1964.

J. M. Mitchell, Jr., "An Analysis of the Fluctuations in the Tropical Stratospheric Wind," [Letter to Editor], *Quarterly Journal of the Royal Meteorological Society*, vol. 90, No. 386, Oct. 1964, p. 481.

J. M. Mitchell, Jr., "Focus on INQUA—The International Association for Quaternary Research," *Bulletin of the American Meteorological Society*, vol. 45, No. 11, Nov. 1964, pp. 688–690.

M. J. Rubin, "Antarctic Weather and Climate," pp. 461–476 in *Research in Geophysics*, vol. 2, "Solid Earth and Interface Phenomena," H. Odishaw, Ed., The M. I. T. Press, Cambridge, Mass., 1964.

M. J. Schroeder, D. W. Krueger, et al., *Synoptic Weather Types Associated with Critical Fire Weather*, Pacific Southwest Forest and Range Experiment Station, Berkeley, Calif., 1964.

R. H. Simpson (with J. S. Malkus), "Hurricane Modification," *Scientific American*, vol. 211, No. 6, Dec. 1964, pp. 27–37.

S. F. Singer, "High Energy Radiation Near the Earth," *Astronautica Acta*, vol. X, Fasc. 1, 1964, pp. 66-80.

W. Spuhler (with R. F. Pengra and D. L. Moe), "Bibliography of South Dakota Climate with Annotations," *Circular 162*, South Dakota Agricultural Experiment Station, Brookings, S. Dak., 1964, 24 pp.

Staff, Stratospheric Meteorology Research Project, "Implementation of the WMO–IQSY STRATWARM Programme," *WMO Bulletin*, vol. 13, No. 4, Oct. 1964, pp. 200–205.

K. Telegadas and R. J. List, "Global History of the 1958 Nuclear Debris and Its Meteorological Implications," *Journal of Geophysical Research*, vol. 69, No. 22, Nov. 15, 1964, pp. 4741–4753.

S. Teweles, "Application of Meteorological Rocket Network Data," *Meteorological Observations Above 30 Kilometers*, National Aeronautics and Space Administration, 1964, pp. 15–35.

(*Continued on page 66*)